Isothermal and Nonisothermal Melt-Crystallization Kinetics of Syndiotactic Polystyrene

QINGYONG CHEN, YINGNING YU, TIANHAI NA, HONGFANG ZHANG, ZHISHEN MO

State Key Laboratory of Polymer Physics and Chemistry, Changchun Institute of Applied Chemistry, Chinese Academy of Sciences, Changchun, 130022, People's Republic of China

Received 16 January 2001; accepted 8 May 2001

ABSTRACT: Analyses of the isothermal and nonisothermal melt kinetics for syndiotactic polystyrene have been performed with differential scanning calorimetry, and several kinetic analyses have been used to describe the crystallization process. The regime II→III transition, at a crystallization temperature of 239°, is found. The values of the nucleation parameter K_g for regimes II and III are estimated. The lateral-surface free energy, $\sigma = 3.24$ erg cm^{-2}, the fold-surface free energy, $\sigma_e = 52.3 \pm 4.2$ erg cm^{-2}, and the average work of chain folding, $q = 4.49 \pm 0.38$ kcal/mol, are determined with the (040) plane assumed to be the growth plane. The observed crystallization characteristics of syndiotactic polystyrene are compared with those of isotactic polystyrene. The activation energies of isothermal and nonisothermal melt crystallization are determined to be $\Delta E = -830.7$ kJ/mol and $\Delta E = -315.9$ kJ/mol, respectively. © 2002 John Wiley & Sons, Inc. J Appl Polym Sci 83: 2528–2538, 2002

Key words: syndiotactic polystyrene; isothermal and nonisothermal melt kinetics; differential scanning calorimetry (DSC); activation energy; regime crystallization

INTRODUCTION

Since the discovery of the successful synthesis of highly stereoregular syndiotactic polystyrene (sPS) in 1986,[1] it has been widely studied in many fields. Most researchers have concentrated on the polymorphic behavior of sPS.[2–4] Four crystalline forms, termed α, β, γ, and δ, have been described. The α and β forms are characterized by chains in the trans-planar (zigzag) conformation, whereas the γ and δ forms contain chains in the $s(2/1)2$ helical conformation.[2] The general pattern is complicated by the fact that both α and β forms can exist with different modifications with different degrees of structural order; two limiting disorder modifications (α' and α'') and two limiting order modifications (β' and β'') have been described.[2–4] However, only few articles have reported the crystallization kinetics of sPS. Cimmino et al.[5] used an optical polarizing microscope to study the isothermal kinetics of sPS. The results indicated that the nucleation rate was very fast and, in fact, faster than the rate for isotactic polystyrene (iPS). Wesson[6] studied the nonisothermal crystallization kinetics of sPS samples with a variety of molecular weights with differential scanning calorimetry (DSC). The results suggested that the crystallization rate depended on the molecular weight. However, the parameters of crystallization kinetics, such as the lateral-surface and fold-surface free energies (σ and σ_e), the average work of chain folding (q), and the activation energies of isothermal and nonisothermal melt crystallization (ΔE), have not been reported until now.

This article is focused on the isothermal and nonisothermal melt-crystallization kinetics of

Correspondence to: Z. Mo (moz@ns.ciac.jl.cn).

Journal of Applied Polymer Science, Vol. 83, 2528–2538 (2002)

DOI 10.1002/app.10192

sPS, as studied with DSC in greater detail, and some of the investigated kinetic parameters of this polymer are compared with those of iPS.

EXPERIMENT

Materials and Preparation

The sPS (Questra F2250) samples were provided by Dow Chemical Co. [weight-average molecular weight (M_w) = 2.2 × 10^5, weight-average molecular weight/number-average molecular weight (M_w/M_n) = 2.4], and the syndiotacticity was about 97% ([rrr] ~ 97%). Its melting temperatures (T_m) and glass-transition temperature (T_g) were about 270 and 100°C, respectively.

DSC

Crystallization kinetics were carried out with a PerkinElmer DSC-7 made by PerkinElmer Corporation (Norwalk, CT) differential scanning calorimeter temperature-calibrated with indium. All DSC runs were performed under a nitrogen purge, and all the sample weights ranged between 8 and 10 mg.

For isothermal melt crystallization, the as-received samples were heated quickly (at 80°C/min) to 320°C, kept in this state for 10 min to eliminate any residual nuclei that might act as seed crystals, and then cooled quickly to the nine designated crystallization temperatures (T_c): 236, 237, 238, 239, 240, 241, 242, 243, and 244°C. Nonisothermal melt-crystallization kinetics were performed by melting at 320°C for 10 min and cooling at constant cooling rates (−2.5, −5.0, −10, −20, and −40°C/min). The exothermal curves of the heat flow as a function of time were recorded and investigated during the melt-crystallization process.

RESULTS AND DISCUSSION

Isothermal Melt-Crystallization Kinetics

In general, the process of isothermal crystallization is composed of two stages: the primary crystallization stage and the secondary crystallization stage. The whole crystallization process is markedly temperature-dependent. If the relative degree of crystallinity increases with increasing crystallization time t, then the Avrami equation[7,8] can be used to analyze the isothermal melt-crystallization process of sPS:

$$1 - X(t) = \exp(-kt^n)$$

$$\log\{-\ln[1 - X(t)]\} = \log k + n \log t \qquad (1)$$

where $X(t)$ is the weight fraction of crystallinity, n is the Avrami index, k is the overall kinetic rate constant, and t is the time of crystallization. In general, the value of n should be an integer between 1 and 4 for different crystallization mechanisms. However, the Avrami exponent is not a straightforward integer, other complex factors are probably involved during the process. The plot of $\log\{-\ln[1 - X(t)]\}$ versus $\log t$ is shown in Figure 1. The figure shows that the curves of higher T_c (i.e., T_c = 244, 243, or 242°C) take on a series of straight lines and that curves of lower T_c tend to deviate from the straight line at a later stage of crystallization. This deviation becomes more obvious with decreasing T_c. The deviation is probably due to the secondary crystallization, which is caused by spherulite impingement in a later stage of the crystallization process.[9,10] From the slope and intercept of the initial portion in Figure 1, the values of n and k have been determined and are listed in Table I. The obtained values of the Avrami exponent vary from 1 to 2 with T_c decreasing from 244 to 236°C, which suggests that the primary crystallization processes should correspond to a two-dimensional circular diffusion-controlled growth for n = 2 or one-dimensional fibrillar growth on the condition that the Avrami exponent is 1 with thermal nucleation[9] for sPS isothermal melt crystallization. The two kinds of crystallization combine to cause an Avrami exponent between 1 and 2. That is, the composition of two-dimensional circular growth will increase with decreasing T_c, and vice versa. The values of the crystallization rate parameter k decrease with increasing T_c because melt crystallization exhibits a temperature dependency characteristic of nucleation-controlled crystallization associated with the proximity of T_m. This is evidence that the process of sPS isothermal melt crystallization is very fast. The result is consistent with the result of Cimmino et al.[5] The crystallization half-time, $t_{1/2}$, is defined as the time at which the extent of crystallization is 50% completed and is determined from the measured kinetic parameters:

$$t_{1/2} = \left(\frac{\ln 2}{k}\right)^{1/n} \qquad (2)$$

Usually, the rate of crystallization, $\tau_{1/2}$, is described as the reciprocal of $t_{1/2}$; that is, $(t_{1/2})^{-1}$

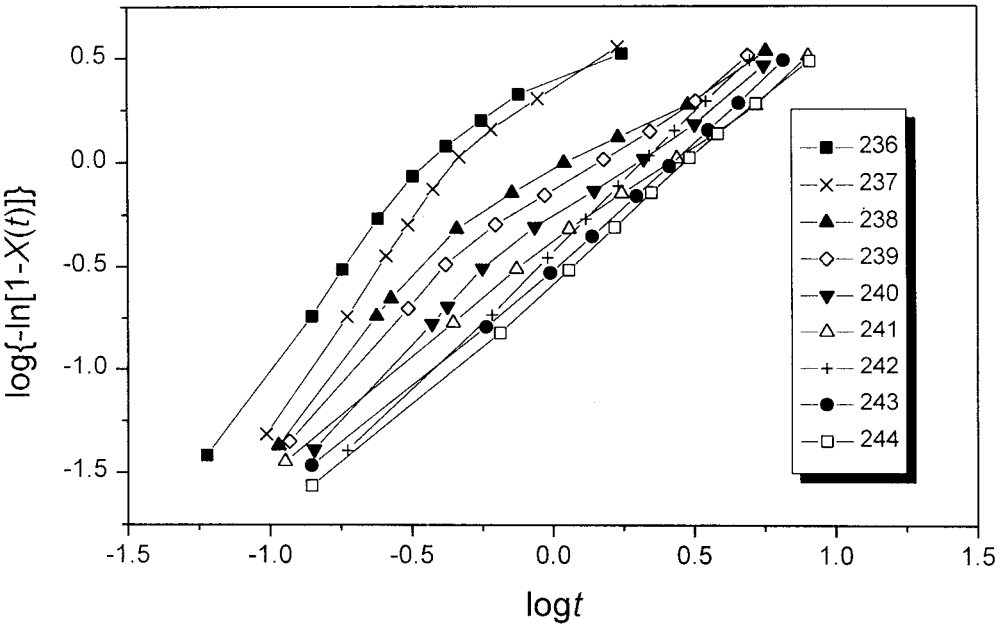

Figure 1 Plot of $\log\{-\ln[1 - X(t)]\}$ versus $\log t$ for the isothermal melt crystallization of sPS at the indicated temperatures.

$= \tau_{1/2}$. The values of k, $t_{1/2}$, and $\tau_{1/2}$ are listed in Table I.

Lin[11] used eq. (1) to calculate the necessary time for maximum crystallization, t_{max}, corresponding to the point at which $dQ(t)/dt = 0$, where $Q(t) = dH_c/dt$ is the heat flow rate; we can determine t_{max} from eq. (1) as follows:

$$t_{max} = \left(\frac{n-1}{nk}\right)^{1/n} \tag{3}$$

With eq. (3), values of $t_{1/2}$, $\tau_{1/2}$, and t_{max} have been calculated, and they are listed in Table I. This is evidence that from 236 to 240°C, t_{max} increases with increasing T_c.

Table I Parameters n, k, t_{max}, $t_{1/2}$, and $\tau_{1/2}$ from Avrami Analysis of Isothermal Melt Crystallization for sPS

T_c (°C)	n	k ($\min^{-n}$)	t_{max} (min)	$t_{1/2}$ (min)	$\tau_{1/2}$ ($\min^{-1}$)
236	1.9	7.9433	0.2292	0.2789	3.5854
237	2.0	5.1051	0.3130	0.3685	2.7139
238	1.5	1.4061	0.3831	0.6241	1.6024
239	1.4	0.8831	0.4124	0.8369	1.1949
240	1.4	0.6546	0.5624	1.0414	0.9603
241	1.1	0.2906	0.3128	1.2038	0.8307
242	1.3	0.3710	0.6534	1.6055	0.6229
243	1.2	0.3165	0.4364	1.9563	0.5089
244	1.1	0.2679	0.5421	2.2524	0.4441

If the crystallization process is thermally activated, the crystallization rate parameter k can be approximately described by an Arrhenius form:[12]

$$K^{1/n} = K_0 \exp(-\Delta E/RT_c)$$

$$\frac{1}{n}\ln k = \ln K_0 - \frac{\Delta E}{RT_c} \tag{4}$$

where K_0 is a temperature-independent pre-exponential factor, ΔE is a total activation energy that can be determined by the slope coefficient of plots of $(1/n)\ln k$ versus $1/T_c$ (Fig. 2), and R is a gas constant. The value of the activation energy for the primary crystallization process of sPS was found to be −830.7 kJ/mol for the isothermal melt crystallization. Because energy must be released during crystallization from the molten fluid to the ordered crystallization phase, the value of ΔE for melt crystallization is negative.

Determination of the Crystal Growth Parameters

Cimmimo[5] et al. proved that sPS crystallizes from the melt according to a spherulite morphology by optical microscopy and that the growth dimensions of the spherulites are very sensitive to T_c and time. Therefore, the spherulitic growth rate

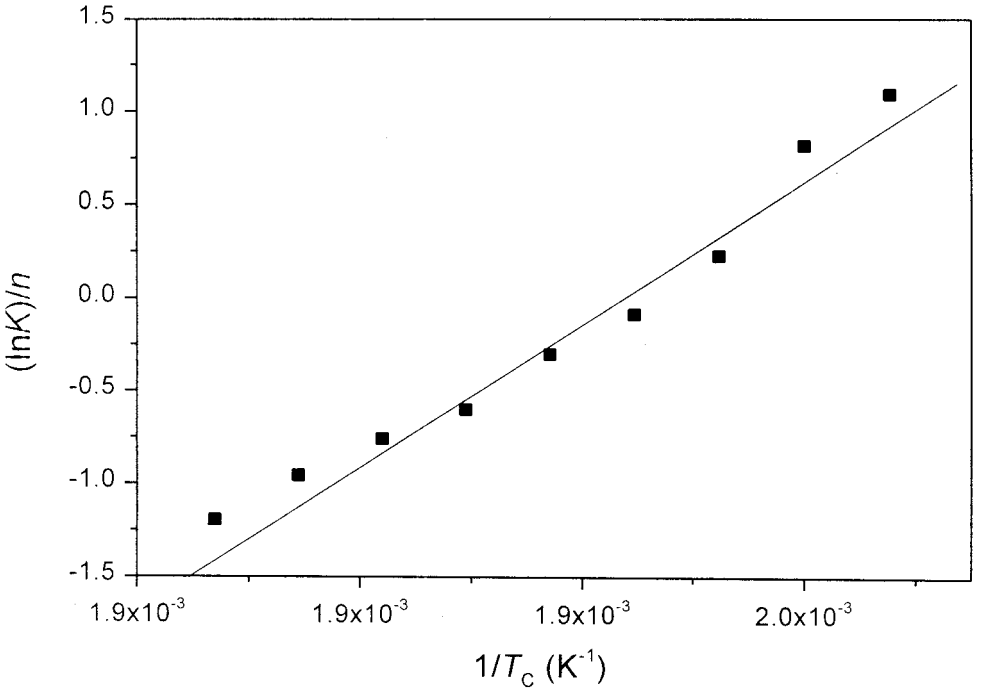

Figure 2 Plot of $(1/n)\ln k$ versus $1/T_c$ for the isothermal melt crystallization of sPS.

(G) of sPS can be determined with the Lauritzen–Hoffman equation[13–16] as follows:

$$G = G_0 \exp\left[-\frac{U^*}{R(T_c - T_\infty)}\right]\exp\left[-\frac{K_g}{T_c(\Delta T)f}\right]$$

$$\ln G + \frac{U^*}{R(T_c - T_\infty)} = \ln G_0 - \frac{K_g}{T_c(\Delta T)f} \qquad (5)$$

where G_0 is a pre-exponential factor, U^* is the transport activation energy and is usually equal to 1500 cal/mol; T_∞ is a hypothetical temperature below which all viscous flow ceases and is universally equal to $T_g - 30$ K;[14] K_g is the nucleation parameter; ΔT is the degree of supercooling and is equal to $T_m^0 - T_c$; and f is a corrector to account for the variation in the bulk enthalpy of fusion per unit volume with temperature and is equal to $2T_c/(T_m^0 + T_c)$. According to He et al.,[17] the majority of the crystal will be β form when the crystallization is higher than 230°C. Because the crystallization we selected is in the range of 236–244°C, here T_m^0 should be taken as the equilibrium melting temperature of the β-form sPS. Considered the correction in the temperature shift, the T_m^0 value of β-form sPS is 551.8 K with Hoffman–Weeks extrapolation.[18] T_g is taken to be 373.25 K (from DSC). From eq. (5), a plot of $\ln G + U^*/R(T_c - T_\infty)$ versus $1/T_c(\Delta T)f$ and the slope of $-K_g$ (Fig. 3) have been obtained. As illustrated in Figure 3, a downward change in the slope indicates that a transition from regime II to regime III can be graphically distinguished. This transition temperature (T_t) corresponds to T_c = 239°C. Moreover, we can obtain the values of $K_{g\ \mathrm{III}} = 3.67 \times 10^5$ and $K_{g\ \mathrm{II}} = 1.58 \times 10^5$ (K^2) from Figure 3. The ratio $K_{g\ \mathrm{III}}/K_{g\ \mathrm{II}}$ is 2.3.

According to refs. 13 and 14, K_g can be defined as follows:

$$K_g = \frac{4b_0\sigma\sigma_e T_m^0}{Bk\Delta h_u^0} \qquad (6)$$

where b_0 is the thickness of a monomolecular layer; σ and σ_e are the lateral and fold-surface free energies of planar-surface lamellae, respectively; k is the Boltzmann constant; and B is 1 in regimes I or III and 2 in regime II. T_m^0 is the equilibrium temperature, and Δh_u^o is the bulk enthalpy of fusion per unit volume for the fully crystalline polymer. Here $\Delta h_u^o = \Delta H_m^o \times \rho_c$, where ΔH_m^o is the heat fusion per unit weight of completely crystalline polymer and is equal to 53.2 J/g.[19] According to the lattice parameters of sPS, the β form is an orthorhombic unit cell with the axes a = 0.881 nm, b = 2.882 nm, and c = 0.505

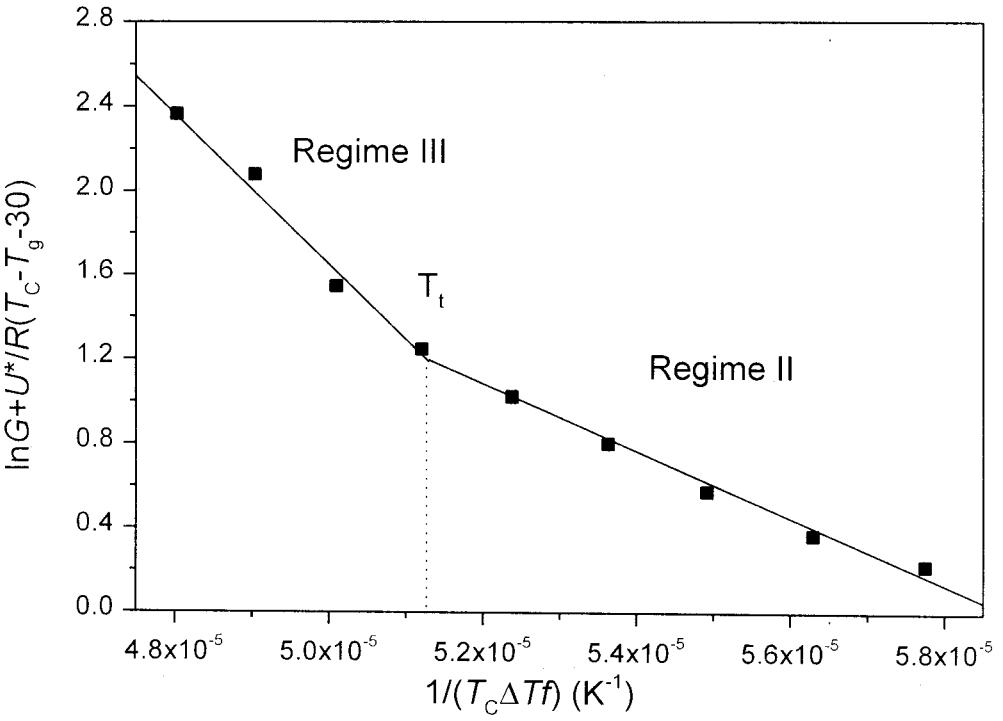

Figure 3 Growth-rate data for the isothermal melt crystallization of sPS.

nm, and this unit cell gives a calculated density of 1.08 g/cm^3.[20] Therefore, $\Delta h_u^o = 53.2 \times 1.08 = 57.5$ J/cm^3. If the crystal growth plane is on the (040) plane, b_0 should be 0.72 nm. Putting these data into eq. (6), we obtain σ and σ_e values of 156 erg cm^{-2} for regime II and 183.2 erg cm^{-2} for regime III, respectively; they are listed in Table II. Obviously, the values appear to be comparable to the values reported for iPS, which were supplied by Edwards and Phillips[21] (listed in Table II).

Following the procedure of Hoffman et al.,[14] we determined σ and σ_e from the value of $\sigma\sigma_e$ as follows:

$$\sigma = \phi(a_0 b_0)^{1/2} \Delta h_u^0 \tag{7}$$

Table II Results of the Isothermal Crystallization Kinetics for sPS and iPS

	sPS		
Parameter	Regime II	Regime III	iPS[a]
T_g (K)	373.25	373.25	363.5
T_m (K)	551.8	551.8	515.2
Δh_u^0 (J/cm^3)	57.5	57.5	91.1
K_g (K^2)	1.58×10^5	3.67×10^5	—
$\sigma\sigma_e$ (erg^2/cm^4)	156.7	183.2	153
σ (erg/cm^2)	3.24	3.24	5.3
σ_e (erg/cm^2)	48.15	56.5	28.8
b_0 (nm)	0.72	0.72	0.55
a_0 (nm)	0.441	0.441	1.28
$A_0 = a_0 b_0$ (nm^2)	31.7×10^{-16}	31.7×10^{-16}	70.5×10^{-16}
q (kcal/mol)	4.11	4.87	4.78

[a] Data from ref. 21.

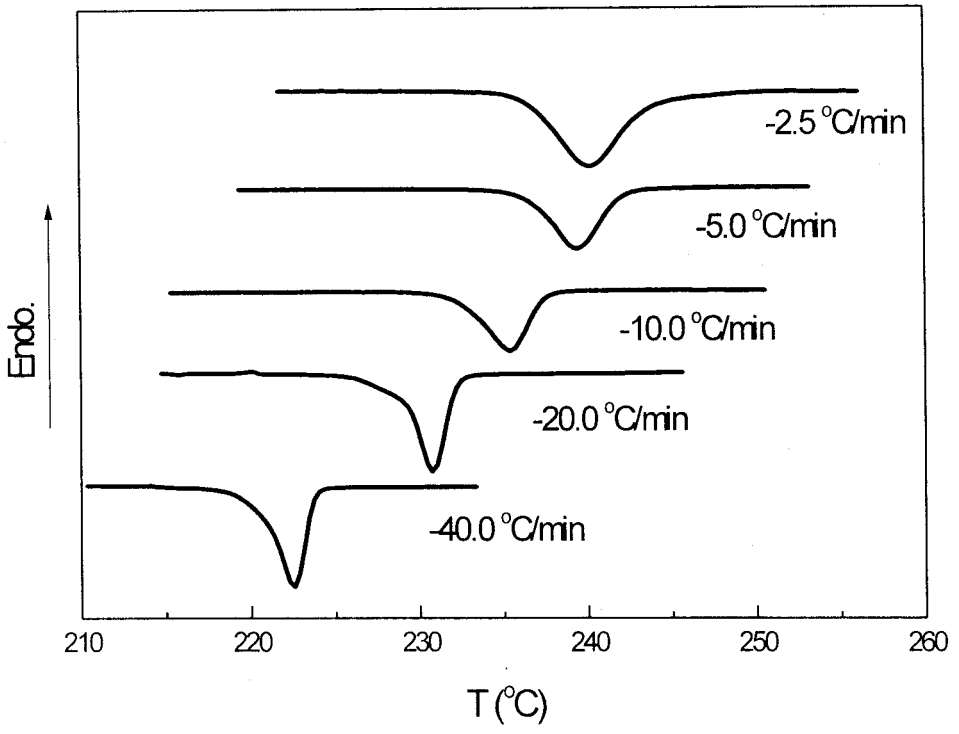

Figure 4 Heat flow versus temperature during the nonisothermal melt crystallization of sPS at different cooling rates as determined by DSC.

$$\sigma_e = \sigma\sigma_e/\sigma \tag{8}$$

where a_0 is the chain width, a_0b_0 is the cross-sectional area per chain molecule, and ϕ is an empirical constant that is usually between 0.1 and 0.3. In general, ϕ is 0.1 for hydrocarbons (e.g., polyolefins) and 0.24 for polyesters [e.g., poly(pivalolactone) and poly(phenylene sulfide)].[22] For sPS, we used $\phi = 0.1$ to estimate the value of σ. According to eq. (8), the value of σ_e can be calculated if the value of $(a_0b_0)^{1/2}$ is known. If the growth plane is the (040) plane, with $a_0 = a/2 = 0.441$ nm and $b_0 = b/4 = 0.72$ nm, the value of σ is 3.24 erg cm^{-2} according to eq. (7). The values of σ_e are, therefore, 48.15 erg cm^{-2} for regime II and 56.5 erg cm^{-2} for regime III according to eq. (8). All the values are listed in Table II.

The work of chain folding per molecular fold can be obtained as the following equation:[14,23]

$$\sigma_e = \sigma_e^0 + q/(2a_0b_0) \tag{9}$$

where σ_e^0 is the value that σ_e would assume if no work were required to form the fold and q is the work required to bend a polymer chain back upon itself, with the conformational constraints imposed on the fold by the crystal structure taken into account. To a reasonable approximation, σ_e^0 may be taken as being roughly equal to σ. Accordingly, eq. (9) is usually written as follows:

Table III Values of T_p, t_{max}, ΔH_c, and $X(t)$ in Nonisothermal Melt Crystallization for sPS

	Φ (°C/min)				
	2.5	5	10	20	40
T_p (°C)	240.6	238.9	235.1	230.6	222.7
t_{max} (min)	4.86	2.68	1.15	0.517	0.404
ΔH_c (J/g)	26.98	27.94	26.89	27.14	27.73
$X(t)$ (%)	54.94	51.69	39.03	38.68	33.56

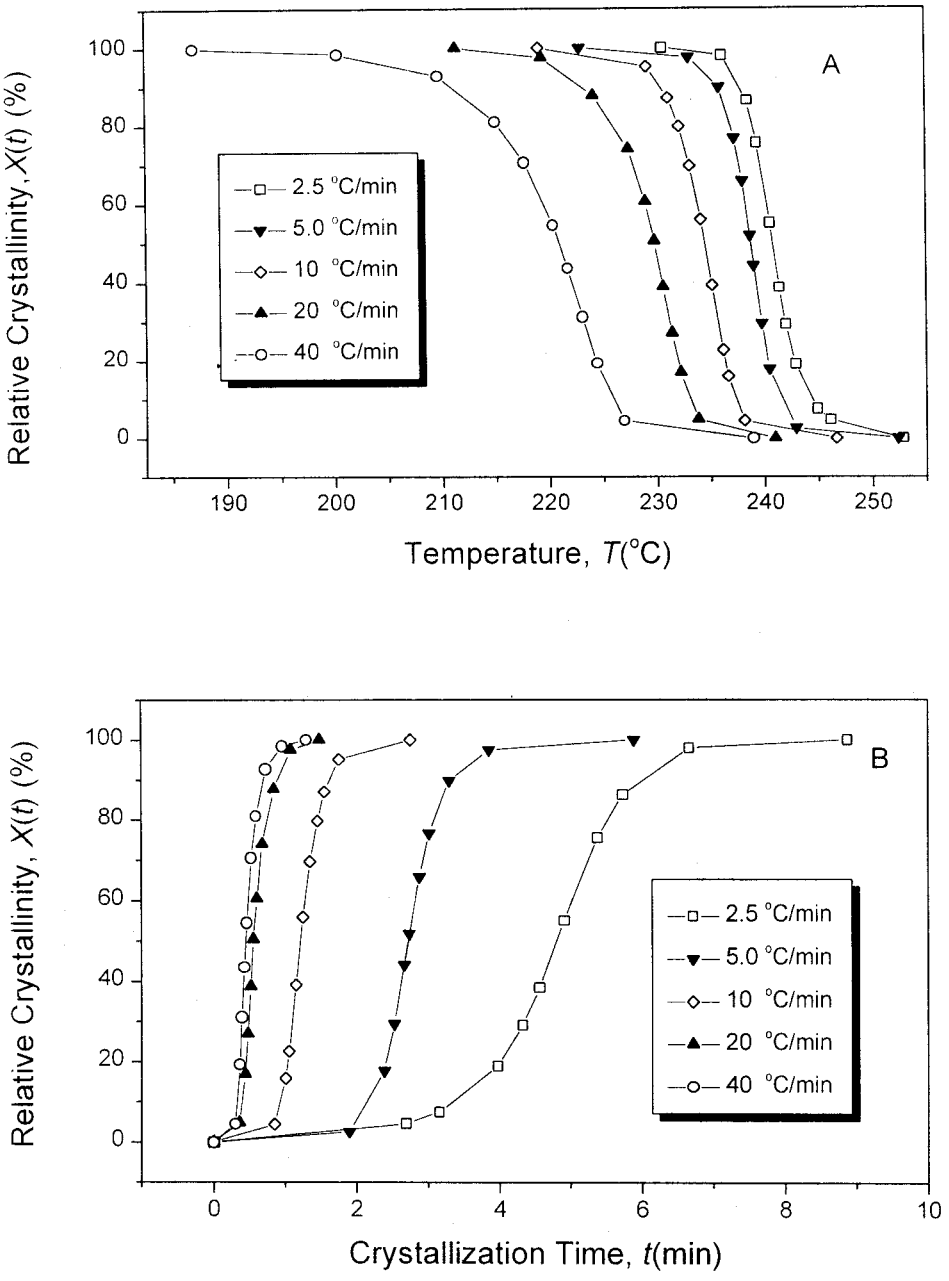

Figure 5 Development of the relative degree of crystallinity with (A) the crystallization time and (B) the temperature for the nonisothermal melt crystallization of sPS.

$$\sigma_e = \sigma + q/(2a_0b_0)$$

$$q = 2a_0b_0(\sigma_e - \sigma) \quad (10)$$

The values of q from eq. (10) for regime II and III crystallization processes have been obtained and are listed in Table II. From Table II, we find that the average value of q for the (040) plane is 4.49 erg cm^{-2}.

To facilitate the comparison of the growth parameters of iPS and sPS, we have also listed them in Table II. The crystal melting temperature is about 543.2 K, about 40 K higher than that of iPS. T_g is 373.25 K, which is about 10 K higher than

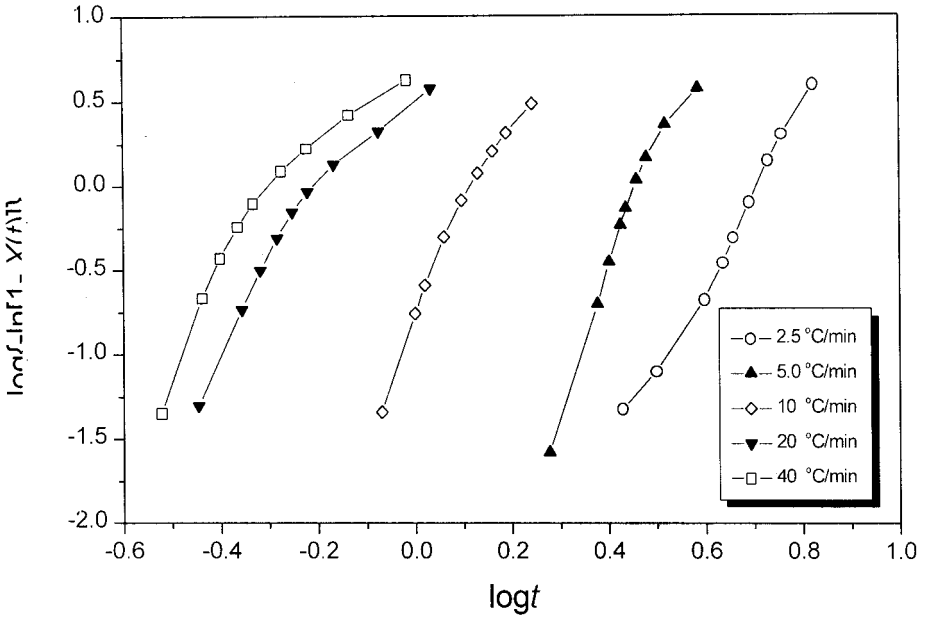

Figure 6 Plot of $\log\{-\ln[1 - X(t)]\}$ versus $\log t$ for the nonisothermal melt crystallization of sPS.

that of iPS. From Table II, we find that the values of A_0 and Δh_u^o of sPS are much smaller than those of iPS. According to eq. (7), this leads to a lower value of σ_e and faster crystallization for sPS. The value of q for growth on the (040) plane of sPS is comparable to that of iPS, although the intramolecular conformations between sPS and iPS are different.

Nonisothermal Melt-Crystallization Kinetics

The Avrami equation is reasonable for analyzing isothermal crystallization kinetics, and its modified forms have been proposed to fit experimental results obtained from nonisothermal crystallization processes. The crystallization exothermic peaks of sPS at various cooling rates Φ are shown in Figure 4. T_p is the peak temperature at which the crystallization rate is maximum, and it is shifted to a lower temperature region when the cooling rate is increased (Fig. 4). The values of the corresponding peak times ($t_{\max}$), T_p at different cooling rates, and crystallization enthalpies (ΔH_c) are listed in Table III. The data indicate that for the maximum T_c (or time), very different rate dependencies exist in the nonisothermal melt crystallization of sPS.

From the DSC data, we calculate the values of the relative crystallinity [$X(t)$] at different crystallization temperatures (T), as shown in Figure 5(A). During the nonisothermal crystallization process, we obtained a series of reversed S curves. A relationship between crystallization T and t is given as follows:

$$t = \frac{|T - T_0|}{\Phi} \tag{11}$$

T_0 is the initial temperature when crystallization begins ($t = 0$). With eq. (11), Figure 5(A) is transformed into Figure 5(B). $X(t)$ can be obtained at various cooling rates from Figure 5(B). Values of $X(t)$ and T_p are shown in Table III.

Mandelkern[24] thought that the primary stage of nonisothermal crystallization could be described by the Avrami equation, which is based on the assumption that T_c is constant:

$$1 - X(t) = \exp[-Z_t t^n]$$

$$\log\{-\ln[1 - X(t)]\} = n \log t + \log Z_t \tag{12}$$

where Z_t is the rate constant in the nonisothermal crystallization process. Jeziorny[25] thought that the values of Z_t determined by eq. (12) should be adequate. Believing Z_t an influence on the cooling

Table IV Parameters n, Z_t and Z_c from Avrami Analysis at the Two Stages of Nonisothermal Melt Crystallization for sPS

Φ (°C/min)	Primary Crystallization Stage			Secondary Crystallization Stage		
	n_1	Z_{t1}	Z_{c1}	n_2	Z_{t2}	Z_{c2}
2.5	4.63	4.26×10^{-4}	1.7×10^{-4}	4.72	5.25×10^{-4}	2.1×10^{-4}
5	9.02	8.1×10^{-5}	1.62×10^{-5}	3.76	2.57×10^{-2}	5.14×10^{-3}
10	7.62	0.164	0.0164	3.59	0.417	0.0417
20	6.02	24.5	1.225	2.33	3.14	0.157
40	6.64	147.9	3.69	2.06	4.73	0.118

or heating rate $\Phi = dT/dt$, Jeziorny assumed that Φ was constant or approximately constant. The final form of the rate parameter characterizing the kinetics of nonisothermal crystallization is given as follows:

$$\log Z_c = \frac{\log Z_t}{\Phi} \tag{13}$$

Drawing the straight line corresponding to $\log\{-\ln[1 - X(t)]\}$ versus $\log t$ with eq. (12), we can obtain the values of the Avrami exponent and the rate parameter Z_t or Z_c from the slope and intercept (Fig. 6). The values of n, Z_t, and Z_c are listed in Table IV.

Ozawa[26] accounted for the effect of the cooling rate Φ on dynamic crystallization by properly modifying the Avrami equation. According to Ozawa's theory, the degree of conversion at temperature T, $C(T)$ can be written as follows:

$$1 - C(T) = \exp[-K(T)/\Phi^m]$$

$$\log\{-\ln[1 - C(T)]\} = -m \log \Phi + \log K(T) \tag{14}$$

where $C(T)$ is the relative degree of crystallinity, m is the Ozawa exponent, and $K(T)$ is the kinetic crystallization rate constant. Drawing the plot of $\log\{-\ln[1 - C(T)]\}$ versus $\log \Phi$ according to eq. (14), we should obtain a series of straight lines, but we did not. The experimental facts indicate that the Ozawa equation is not suitable for describing the kinetics in the nonisothermal crystallization process of sPS. In recent years, a con-

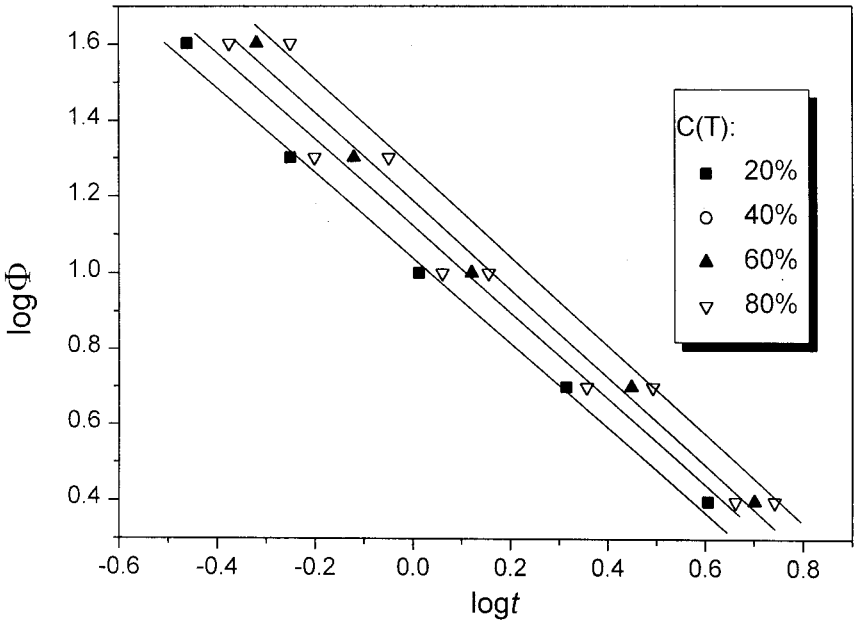

Figure 7 Plot of $\log \Phi$ versus $\log t$ of sPS for various values of $C(T)$.

venient kinetic method proposed by our research group has been adopted to deal with the nonisothermal data of many polymer systems.[27–29] A convenient method modified by the combination of the Avrami equation and the Ozawa equation is

$$\log \Phi = \frac{1}{m} \log[K(T)/Z_t] - \frac{n}{m} \log t$$

$$\log \Phi = \log F(T) - a \log t \qquad (15)$$

where the parameter $F(T) = [K(T)/Z_t]^{1/m}$ refers to the value of the cooling rate, which is chosen at the unit crystallization time when the measured system has reached a certain degree of crystallinity, and a is the ratio of the Avrami exponent n to the Ozawa exponent m (i.e., $a = n/m$).[28] At a certain degree of crystallinity of sPS, the plot of $\log \Phi$ versus $\log t$ according to eq. (15) is shown in Figure 7. It gives a series of straight lines at a given relative degree of crystallinity, and the kinetic parameter $F(T)$ and the exponent a can be estimated by the intercept and slope of these straight lines, respectively. The results for a and $F(T)$ are listed in Table V. It is apparent that $F(T)$ increases systematically with an increasing relative degree of crystallinity, but the values of a are almost constant, about 1.0, indicting that the Avrami exponent n is equal to the Ozawa exponent m.

Table V Values of a and $F(T)$ and C (T) from Equation of sPS

	$C(T)$ (%)			
	20	40	60	80
a	0.9405	1.114	1.032	1.057
$F(T)$	0.896	1.13	0.866	0.839

For nonisothermal melt crystallization, the activation energy of crystallization was derived from the Kissinger equation[30] in the following form:

$$[d(\ln \Phi/T_p^2)]/[d(1/T_p)] = -\Delta E/R \qquad (16)$$

where R is the universal gas constant and the rest of the parameters have the aforementioned meanings [the slope of a plot of $\log(\Phi/T_p^2)$ versus $1/T_p$]. In this way, we obtain a line with a good linear relation in Figure 8; the slope is $d[\log \Phi/T_p^2]/[d(1/T_p)]$, and ΔE is -315.9 kJ/mol.

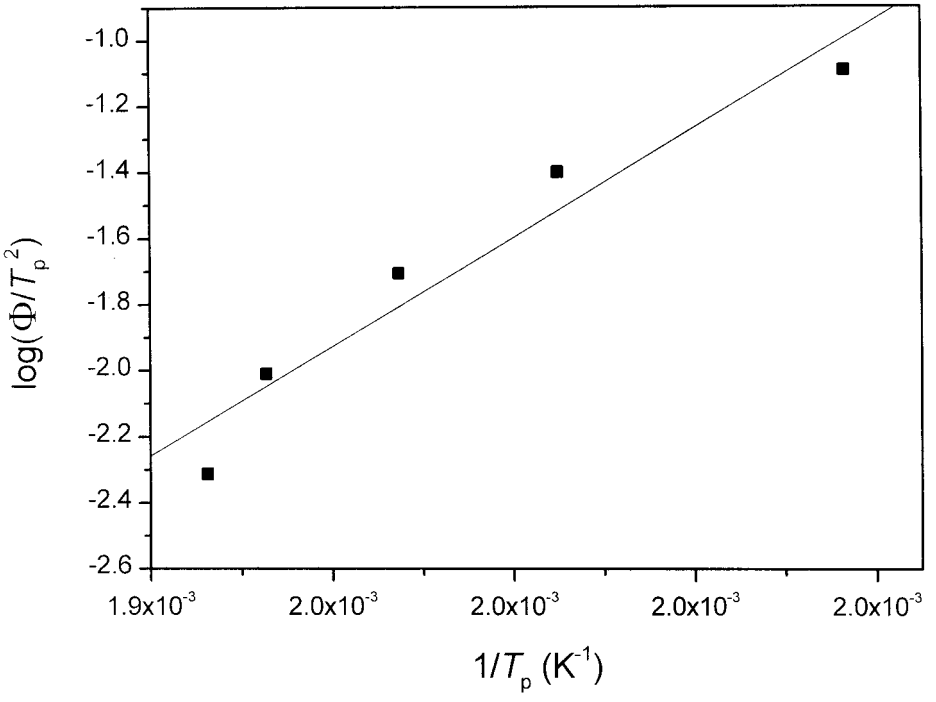

Figure 8 Kissinger plot for the determination of the activation energy of the nonisothermal melt crystallization of sPS.

CONCLUSION

A systematic study of the isothermal and nonisothermal melt-crystallization kinetics of sPS has been carried out with DSC techniques. On the basis of an Avrami analysis, either isothermal melt crystallization at a lower value of T_c (i.e., T_c = 236–241°C) or nonisothermal melt crystallization is composed of primary and secondary stages, but no secondary crystallization exist in isothermal melt-crystallization processes at higher values of T_c. A convenient method has been applied to characterize the nonisothermal melt crystallization of sPS by the combination of the Avrami equation with the Ozawa equation, and the result shows this method is also fit for describing the nonisothermal melt-crystallization process. The Lauritzen–Hoffman nucleation theory has been applied to linear growth-rate data of the sPS isothermal melt crystallization. A transition from regime II to regime III has been observed at T_c = 239°C. The values of $K_{g\ III}$ and $K_{g\ II}$ and the ratio $K_{g\ III}/K_{g\ II}$ have been estimated. By supposing that the (040) plane is the growth plane, we have evaluated growth parameters such as the lateral-surface free energy (σ). the fold-surface free energy (σ_e), and the average work of chain folding (q). These parameters of sPS have been compared with those of iPS.

The research was supported by the Key Projects of the National Natural Science Foundation of China and subsidized by the Special Funds for State Basic Research Projects.

REFERENCES

1. Ishihara, N.; Seimiya, T.; Kuramoto, M.; Uoi, M. Macromolecules 1986, 19, 2464.
2. Guerra, G.; Vitagliano, V. M.; De Rosa, C.; Petraccone, V.; Corradini, P. Macromolecules 1990, 23, 1539.
3. De Rosa, C.; Rapacciuolo, M.; Guerra, G.; Petraccone, V.; Corradini, P. Polymer 1992, 33, 1423.
4. De Rosa, C.; Guerra, G.; Petraccone, V.; Corradini, P. Polym J 1991, 23, 1435.
5. Cimmino, S.; Pace, E. D.; Martuscelli, E.; Silvestre, C. Polymer 1991, 32, 1080.
6. Wesson, R. D. Polym Eng Sci 1994, 34, 1157.
7. Avrami, M. J Chem Phys 1939, 7, 1103.
8. Avrami, M. J Chem Phys 1940, 8, 212.
9. Wunderlich, B. Macromolecular Physics; Academic: New York, 1977; Vol. 2.
10. Liu, J. P.; Mo, Z. S. Chin Polym Bull 1991, 4, 199.
11. Lin, C. C. Polym Eng Sci 1983, 23, 113.
12. Cebe, P.; Hong, S. D. Polymer 1986, 27, 1183.
13. Hoffman, J. D. Soc Plast Eng Trans 1964, 4, 315.
14. Hoffman, J. D; Davis, G. T.; Lauritzen, J. I. Treatise on Solid State Chemistry; Hannay, H. B., Ed.; Plenum: New York, 1975; Vol. 3, Chapter 6.
15. Lauritzen, J. I.; Hoffman, J. D. J Appl Phys 1973, 44, 4340.
16. Wang, T. T.; Nish, T. Macromolecules 1977, 19, 421.
17. Bu, W. S.; Li, Y. Y.; He, J. S.; Zeng, J. J. Macromolecules 1999, 32, 7724.
18. Ho, R. M.; Lin, C. P.; Tsai, H. Y.; Woo, E. M. Macromolecules 2000, 33, 6517.
19. Pastor, A. J.; Landes, B. G.; Karjala, B. G. Thermochim Acta 1991, 177, 187.
20. Chatani, Y.; Shimane, Y.; Ijitsu, T.; Yukinari, T. Polymer 1993, 34, 1625.
21. Edwards, B. C.; Phillips, P. J. Polymer 1974, 15, 351.
22. Roitman, D. B.; Marand, H.; Miller, R. L.; Hoffman, J. D. J Phys Chem 1989, 93, 6919.
23. Lauritzen, J. I. J Appl Phys 1973, 44, 4353.
24. Mandelkern, L. Crystallization of Polymers; McGraw Hill: New York, 1964.
25. Jeziorny, A. Polymer 1987, 19, 1142.
26. Ozawa, T. Polymer 1971, 12, 150.
27. Liu, T. X.; Mo, Z. S.; Wang, S. E.; Zhang, H. F. Polym Eng Sci 1997, 37, 568.
28. Liu, S. Y.; Yu, Y. Y.; Cui, Y.; Zhang, H. F.; Mo, Z. S. J Appl Polym Sci 1998, 70, 2371.
29. Qiu, Z. B.; Mo, Z. S.; Zhang, H. F.; Sheng, S. R.; Song, C. S. J Macromol Sci Phys 2000, 39, 873.
30. Kissinger, H. E. J Res Natl Bur Stand 1956, 57, 217.